BMC Complementary Medicine and Therapies

RESEARCH

Open Access

Potential mechanism prediction of indole-3-propionic acid against diminished ovarian reserve via network pharmacology, molecular docking and experimental verification

Ahui Liu[1,2†], Zhijun Liu[4†], Haofei Shen[1,2,3†], Wenjing Du[1,2,3], Yanbiao Jiang[1,2], Liyan Wang[2,3], Rui Zhang[2,3], Panpan Jin[2,3*] and Xuehong Zhang[2,3*]

Abstract

Background Oxidative stress (OS) is one of the major causes of ovarian aging and dysfunction. Indole-3-propionic acid (IPA) is an indole compound derived from tryptophan with free radical scavenging and antioxidant properties, and thus may have potential applications in protecting ovarian function, although the exact mechanisms are unknown. This study aims to preliminarily elucidate the potential mechanisms of IPA that benefit ovarian reserve function through network pharmacology, molecular docking, and experimental verification.

Methods The related protein targets of IPA were searched on SwissTargetPrediction, TargetNet, BATMAN-TCM, and PharmMapper databases. The potential targets of diminished ovarian reserve (DOR) were identified from OMIM, GeneCards, DrugBank, and DisGeNET databases. The common targets were uploaded directly to the STRING database to construct PPI networks. We then performed GO and KEGG enrichment analysis on the targets. Subsequently, molecular docking and molecular dynamics simulation were used to validate the binding conformation of IPA to candidate targets. Furthermore, we carried out in vitro experiments to validate the prediction results of network pharmacology.

Results We identified a total of 61 potential targets for the interaction of IPA with DOR. The PPI network topological parameter analysis yielded 13 hub genes for DOR treatment. The GO biological process enrichment analysis identified 293 entries, mainly enriched in aging, signal transduction, response to hypoxia, negative regulation of apoptotic process, and positive regulation of cell proliferation. The KEGG enrichment analysis mainly included lipid and atherosclerosis, progesterone-mediated oocyte maturation, AGE-RAGE, relaxin, estrogen, and other signaling pathways. The molecular docking further revealed the direct binding of IPA with six hub proteins including NOS3, AKT1, EGFR,

†Ahui Liu, Zhijun Liu and Haofei Shen these authors contributed equally to this work.

*Correspondence:
Panpan Jin
331999640@qq.com
Xuehong Zhang
zhangxueh@lzu.edu.cn
Full list of author information is available at the end of the article

PPARA, SRC, and TNF. In vitro experiments showed that IPA pretreatment attenuated H_2O_2-induced cellular oxidative stress damage, while IPA exerted cytoprotective and antioxidant damage effects by regulating the six hub genes and antioxidant proteins.

Conclusion We systematically illustrated the potential protective effects of IPA against DOR through multiple targets and pathways using network pharmacology, and further verified the cytoprotective effect and antioxidant properties of IPA through in vitro experiments. These findings provide new insights into the targets and molecular mechanisms whereby IPA improves DOR.

Keywords Indole-3-propionic acid, Diminished ovarian reserve, Network pharmacology, Molecular docking, Molecular dynamics simulation, Experimental verification

Introduction

Diminished ovarian reserve (DOR) is a common gynecological endocrine disorder that refers to a reduction in the number of follicles and the quality of oocytes in the ovary. Without timely intervention and treatment, it can further progress to premature ovarian failure (POF), which seriously affects the reproductive health and quality of life of women [1]. The etiology and pathogenesis of DOR have not been clarified, its etiology may be associated with age, genetics, enzyme deficiencies, autoimmune damage, and certain ovarian destructive factors (such as radiotherapy, chemotherapy, surgery, infection, etc.) [2]. In recent years, it has been found that oxidative stress (OS) is one of the most significant causes of impaired ovarian function, which can lead to reproductive endocrine dysfunction, induce apoptosis of granulosa cells, and then affect follicular atresia [3, 4]. To counteract the negative effects of oxidative damage, the human body needs to produce endogenous antioxidants or obtain exogenous antioxidants from foods [5].

As an essential amino acid, tryptophan (TRP) must be obtained from the diet and plays an important regulatory role in many metabolic functions in the body. The kynurenine, serotonin/melatonin, and indole pathways are the three metabolic pathways of TRP, all of these pathways have been reported to be correlated with aging [6, 7], and its important representative is melatonin. Melatonin is widely known as an anti-aging agent that has been reported in many studies and has also been tried in assisted reproductive technology to improve oocyte quality and ovarian function [8, 9]. Notably, indole-3-propionic acid (IPA) is an indole metabolite produced by gut microbiota metabolizing TRP and has the same highly resonance stable heterocyclic aromatic ring structure as melatonin [10]. In vitro experiments have shown that IPA is more effective than melatonin at scavenging hydroxyl radicals and preventing oxidative damage to membrane lipids [11, 12]. Over the last twenty years, IPA has been identified to play a neuroprotective role in the brain due to its powerful cytoprotective properties as an antioxidant [13, 14]. In recent years, studies have found significant reductions in IPA levels in several diseases and pathogenic states including diabetes [15], non-alcoholic fatty liver disease [16], colitis [17], and obesity [18]. Additionally, the supplementation of IPA has also been shown to inhibit the synthesis of pro-inflammatory factors as well as to protect cells from the effects of OS and lipid peroxidation [19, 20].

IPA has been reported to be absorbed by intestinal epithelial cells and circulated to multiple organ targets in the body, thus exerting corresponding biological functions [21]. Interestingly, our previous study found that IPA levels in follicular fluid (FF) were significantly lower in DOR patients than in the control group, and consider that IPA may be a potential biological marker for DOR or an ovarian protector [22]. Similarly, Ruebel et al. found that the concentration of IPA in the FF of obese infertile women was significantly lower than that of infertile women with normal weight [23], and considered that obesity alters the microenvironment of follicular development, causing increased OS and decreased antioxidant capacity, and that IPA may be one of the substances exerting antioxidant effects in the ovary. Overall, it is reasonable to assume that IPA may play a potential role in improving ovarian function, however, the biological pathways and specific mechanisms of its action are still unclear.

Network Pharmacology is the result of integrating multidisciplinary basic theories and research methods from medicine, biology, computer science, and bioinformatics, which can systematically reflect the mechanisms of drug intervention [24]. Moreover, network pharmacology does not study the interactions between a single molecule and a single target in isolation but enables the investigation of multi-target, multi-pathway synergistic relationships between compounds, genes, and diseases, thus it makes possible the discovery of natural drugs with novel mechanisms of action and potential therapeutic value [25].

This study aimed to reveal the predictive targets and potential therapeutic mechanisms of IPA on DOR based on the method of network pharmacology and molecular docking, subsequently, based on these analyses, we performed experimental validation using an in vitro model

that simulates DOR. Figure 1 illustrates the workflow of the study.

Materials and methods

Identification of IPA targets

The chemical structure and Canonical SMILES information of the IPA was found in the PubChem database (https://pubchem.ncbi.nlm.nih.gov/) [26]. Subsequently, four online public databases including SwissTargetPrediction (http://www.swisstargetprediction.ch/) [27], TargetNet (http://targetnet.scbdd.com/home/index/) [28], BATMAN-TCM (http://bionet.ncpsb.org/batman-tcm/) [29], and PharmMapper (http://www.lilab-ecust.cn/pharmmapper) [30] were employed to predict the IPA potential targets by limiting the species with "Homo sapiens". All obtained gene names were standardized through the UniProt database (http://www.uniprot.org/) [31].

Identify targets for DOR

The DOR-associated targets were collected from OMIM (http://www.omim.org) [32], GeneCards (https://www.genecards.org/) [33], DrugBank (https://go.drugbank.com/) [34], and DisGeNET databases (https://www.disgenet.org/) [35], with the theme of diminished ovarian reserve as a search term. In the Genecards database, the higher the score value the closer the correlation between the target and the disease, therefore, set the DOR-related targets with a gene-disease score more than the median [25]. The targets obtained from the four databases were combined, and the repetitions were removed to construct DOR-related targets.

IPA-DOR protein–protein interaction (PPI) network

Venn diagrams were drawn to identify the intersection of the IPA and DOR targets using the online website (https://bioinfogp.cnb.csic.es/tools/venny/). Afterward, the common targets were submitted to construct a PPI network on the STRING (Version 11.5) database (https://string-db.org/) [36]. The species was set as "Homo sapiens", and the minimum interaction threshold was set to "high confidence" (> 0.7). The PPI and component-target genes-disease (CTD) networks were then visualized by Cytoscape v3.9.1. In addition, we used the CentiScaPe plug-in to analyze the degree centrality (DC), closeness centrality (CC), and betweenness centrality (BC). The targets that all meet the average of greater than DC, CC, and BC were considered the core genes.

GO and KEGG pathway enrichment

The common targets were submitted to the DAVID online tool (https://david.ncifcrf.gov) for Gene ontology (GO) annotations and Kyoto Encyclopedia of Genes and Genomes (KEGG) pathway analysis [37]. The data were visualized using ggplot2 packages in R 4.1.2 software [38].

Screening function modules

The Molecular Complex Detection (MCODE) [39], a Cytoscape plugin, was used to explore functional modules in the PPI network. The screening criteria were set according to the system. The proteins of each module were then subjected to GO and KEGG enrichment analysis.

Molecular docking analysis

Target protein and ligand preparation

The 2D structure of IPA ligand as SDF files were downloaded from PubChem and converted into mol2 format using ChemBio3D Ultra 21.0. The structures of target protein receptors were downloaded from the PDB database (https://www.rcsb.org/structure) and were processed with PyMOL (version 2.5) to remove water and unnecessary ligands.

Molecular docking

AutoDock Tools 1.5.6 was used to convert ligands and proteins into the pdbqt file format [40], Gasteiger charges were calculated and the binding pocket was defined. Molecular docking calculations were performed using AutoDock Vina [41], and the docking poses were visualized using PyMOL. Finally, the binding strength and activity of the core targets and the ligand were evaluated by the docking score.

Molecular dynamics simulation

After molecular docking, the IPA and NOS3 with the strongest binding activity were selected for molecular dynamics (MD) simulation. The MD simulation was performed with GORMACS package (version 2022.3) [42], and parameter files were obtained by selecting the AMBER99SB force field using GORMACS for target proteins and the GAFF force field for ligand molecules. Before the simulation, the complex was solvated by placing it into the center of a cubic box filled with water, and the atoms of the complex were allowed to have a minimum distance of 1.0 nm from the boundary of the box, while Na^+ and Cl^- were added to neutralize the charge of the whole system. The MD simulation system was first energy minimized using the steepest descent method, and then carried out the isothermal isovolumic ensemble (NVT) equilibrium and isothermal isobaric ensemble (NPT) equilibrium for 100,000 steps, respectively, with the coupling constant of 0.1 ps and duration of 100 ps. Finally, a free MD simulation was performed with a run time for 100 ns and a time step set to 2 fs. We calculated

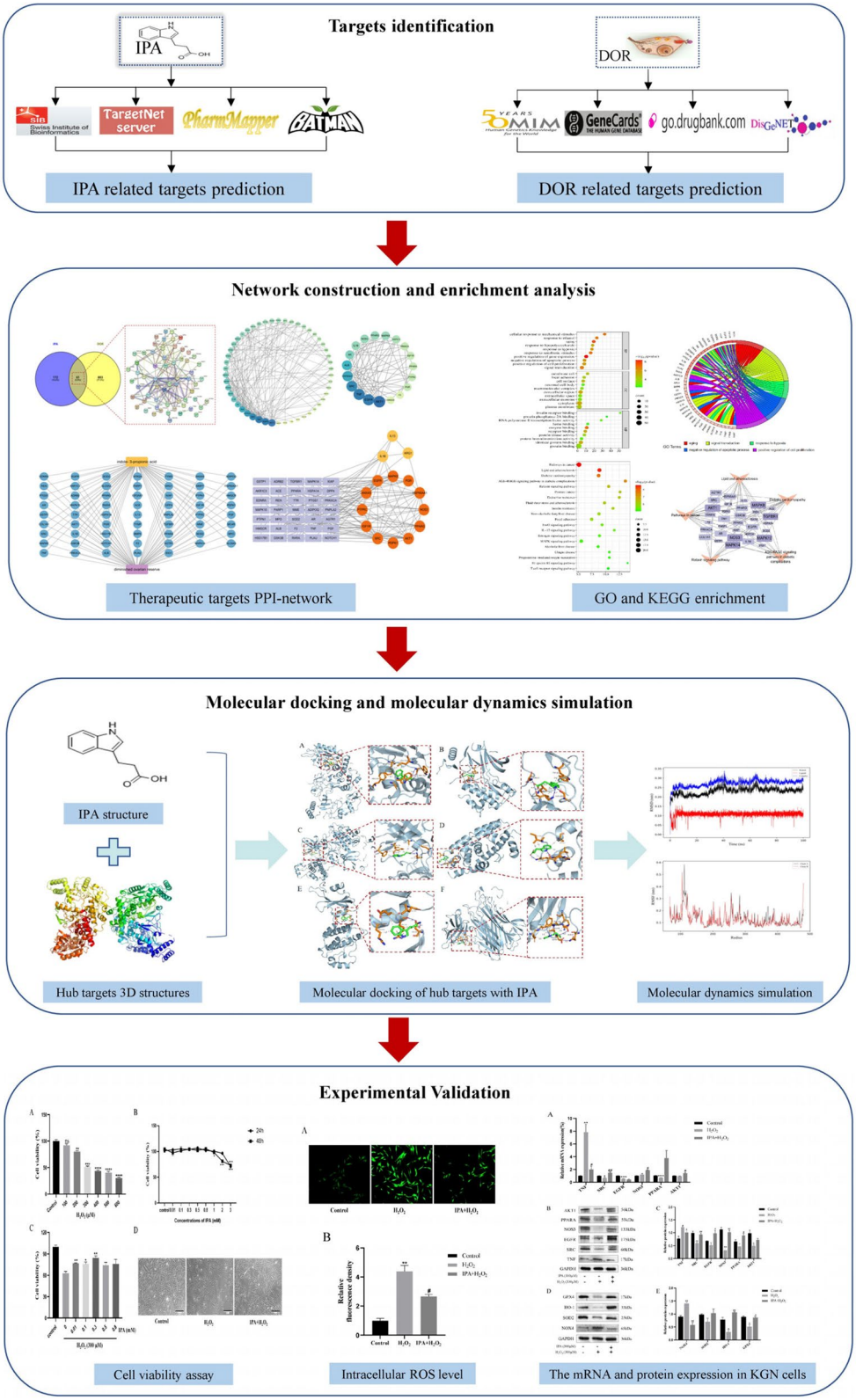

Fig. 1 Workflow chart

the root mean square deviation (RMSD) and root mean square fluctuation (RMSF) values to assess the stability and flexibility of the complexes. The binding free energy values and interactions of ligands with proteins were calculated by the MM/GBSA method [43].

Cell culture and viability assay

The commercially available human ovarian granulosa tumor cell line (KGN) (Cat No.: CL-0603) was purchased from Procell Life Science & Technology Co., Ltd (Wuhan, China). The cell line was cultured in DMEM/F-12 (Gibco) supplemented with 10% FBS and 1% penicillin/streptomycin at 37 °C in a CO_2 incubator. KGN cells were plated into 96-well plates at a density of 8×10^3 cells per well, then treated with various concentrations of hydrogen peroxide (H_2O_2, Boster Biological Technology Co. Ltd) and IPA (Sigma-Aldrich, St. Louis, MO, USA) for the indicated times. Subsequently, 10 μL cell counting kit-8 (CCK8, Coolaber, China) reagent was added to each well and incubated at 37 °C for 2 h to detect cell viability. The absorbance values were read at 450 nm in a microplate reader (Tecan, Grodig, Austria, GmbH).

Reactive oxygen species (ROS) detection

Levels of intracellular ROS were determined by ROS assay kit (Beyotime, China). KGN cells were seeded in 6-well plates and incubated overnight. The cells were pre-treated with the indicated concentrations of IPA for 24 h, followed by treatment with the indicated concentrations of H_2O_2 for 2 h. According to the instructions, cells were washed with PBS and then incubated with serum-free medium containing 10 μM DCFH-DA solution for 30 min at 37 °C in a cell culture incubator. After washing again with the same medium, the level of ROS production was observed by fluorescence microscopy.

Real-time quantitative PCR (RT- qPCR) analysis

The mRNA expression levels of NOS3, AKT1, EGFR, PPARA, SRC, and TNF were measured using RT-qPCR. Total cellular RNA was extracted using the Trizol reagent (Coolaber, China), and cDNA was generated using a reverse transcription kit (Servicebio, Wuhan, China). qPCR was carried out using SYBR Green (Servicebio, Wuhan, China) according to the manufacturer's protocol. All primer sequences were synthesized by Shanghai Sangon Biotechnology Co., Ltd., and were listed in Supplementary Table 1.

Western blot analysis

Western blot (WB) method was performed to detect the expression levels of six hub targets and antioxidant proteins in KGN cells. Cells were harvested and lysed, and the protein concentration was evaluated by the BCA reagent kit (Coolaber, China). Thereafter, protein samples (30μg) were separated by 10–12% SDS-PAGE and then transferred into PVDF membranes (Millipore, USA). The membranes were blocked with 5% defatted milk for 2 h at room temperature and then incubated with primary antibodies overnight at 4 °C. In addition, to detect multiple proteins on the same membrane, we trimmed the membrane according to the protein molecular weight range in the instructions prior to hybridization with the antibody, and all original blots as well as replicates are provided in Supplementary Fig. 1. Next, membranes were washed three times with TBST and then incubated with HRP-conjugated secondary antibodies for 2 h at room temperature. After washing again, the membranes were incubated with enhanced chemiluminescence (ECL) solution (Xin Saimei, China) and imaged by the Bio-Rad system (Bio-Rad, USA). Finally, the Image-J software was used to calculate the relative densities of protein bands. Primary antibodies against NOS3 (WL01789), AKT1 (WL01652), EGFR (WL0682a), PPARA (WL00978), SRC (WL01570), and TNF (WL01581) were obtained from Wanleibio (Shenyang, China). Primary antibodies against GPX4 (T56959) was obtained from Abmart (Abmart, Shanghai), NOX4 (14,347–1-AP), SOD2 (24,127–1-AP), HO-1 (10,701–1-AP), GAPDH (10,494–1-AP), and HRP-Goat-Anti-Rabbit IgG (H + L) (SA00001-2) were obtained from Wuhan Sanying Biotechnology (Wuhan, China).

Statistical analysis

Data are represented as means ± SD with the student's t-test used to calculate statistical significance between groups. $P < 0.05$ were considered significant.

Results

The targets of indole-3-propionic acid and diminished ovarian reserve

By searching SwissTargetPrediction, TargetNet, BATMAN-TCM, and PharmMapper databases, a total of 233 IPA targets were obtained after the removal of the duplicates (Supplementary 1). The potential targets of DOR were identified from OMIM, GeneCards, DrugBank, and DisGeNET databases. The keyword for the search was "diminished ovarian reserve." Specifically, a total of 272 DOR-related targets were obtained from the OMIM database, 18 targets from the DrugBank database, and 43 targets from the DisGeNET database. Furthermore, we obtained a total of 1218 targets from the GeneCards database, the maximum target relevance score was 201.83, the minimum was 0.26, and the median was 3.15, thus we obtained 609 targets with scores greater than 3.15. Target genes from four databases were merged and duplicates were removed, 864 DOR-related targets in total were identified at last (Supplementary 2).

Identification of the potential therapeutic targets by PPI network

Based on the target preparation above, 61 potential IPA targets for treating DOR were identified (Fig. 2A). PPI network diagrams were established through the STRING database (Fig. 2B). Then, the network topological parameters were analyzed to highlight the hub genes. As a result, thirteen hub genes were found according to the average values for DC, CC, and BC, which were 6.65, 0.008814125, and 67.96, respectively (Supplementary 3). These hub genes are AKT1, TNF, EGFR, SRC, HSP90AA1, ALB, AR, NOS3, PPARG, MAPK8, PPARA, PTPRC, F2 (Fig. 2C and Table 1). Additionally, an IPA-target genes-DOR network was constructed to visualize and clarify the pharmacological potential of IPA against DOR (Fig. 2D). In detail, the blue circle nodes represent 61 common target genes, and another two rectangle nodes represent IPA (orange) and DOR (purple), respectively.

GO and KEGG pathway enrichment analysis

GO enrichment analysis

GO enrichment analysis of the 61 common targets was performed to explore their biological characteristics, which showed that 293 GO terms in the biological processes (BP), 33 terms in the cellular components (CC), and 56 terms in the molecular functions (MF) ($P < 0.05$). The top 10 GO items were selected based on enriched gene numbers and p-values (Fig. 3A). After the screening process, a chord plot was drawn for the top 5 of the biological processes (Fig. 3B). As can be seen in the top 5 enriched BPs, the effects of IPA against DOR were mechanistically linked to aging, signal transduction, response to hypoxia, negative regulation of apoptotic process, and positive regulation of cell proliferation. Notably, ten of the thirteen hub targets were also enriched in the top 5 enriched BPs, including AKT1, TNF, EGFR, SRC, HSP90AA1, ALB, AR, PPARG, MAPK8, PPARA, and F2. Molecular functions are primarily connected with a series of binding activities including enzyme binding, identical protein binding, receptor binding, protein binding, and protein kinase activity. Additionally, different cellular components such as cytoplasm, plasma membrane, extracellular region, and focal adhesion were highlighted by the GO annotations.

KEGG pathway analysis of key targets in DOR treatment

We performed a KEGG enrichment analysis for 61 therapeutic targets. A total of 102 KEGG pathways were identified with a p-value < 0.05. The top 20 most significant pathways related to the treatment of DOR were displayed (Fig. 3C), which mainly contained pathways in cancer, lipid and atherosclerosis, diabetic cardiomyopathy, AGE-RAGE signaling pathway in diabetic complications, and relaxin signaling pathway. Additionally, we connected these 5 major KEGG-enriched pathways and cross-target genes and visualized the results (Fig. 3D), suggesting these pathways may be targets for the therapeutic role of IPA in DOR. Next, to further explore the signaling pathway of IPA against DOR, the 13 hub genes were subjected to KEGG enrichment analysis (Supplementary 4). We also performed a pathways-targets network on the top 5 pathways enriched by KEGG (Fig. 3E), which highlighted the involvement of hub target-related pathways.

Function modules-based network analysis

To further confirm the biological function of the common targets for IPA against DOR, we used the MCODE plug-in to detect the modules of the PPI network and thus found 2 closely interconnected gene clusters (cluster 1 and cluster 2) with the highest clustering scores. Cytoscape was used to draw the cascade map of modules (Fig. 4A). Furthermore, GO and KEGG analysis were performed on the two clusters (Supplementary 5), and the relationships between the top 5 pathways and targets were visualized for each of the 2 clusters (Fig. 4B, C;Table 2). The main KEGG pathways enriched were lipid and atherosclerosis, estrogen signaling pathway, progesterone-mediated oocyte maturation, relaxin signaling pathway, FoxO signaling pathway, and IL-17 signaling pathway.

Molecular docking

Molecular docking methods were performed to examine the binding affinity of IPA to its 13 potential hub targets. It is widely accepted that the more stable the ligand-receptor binding conformation, the lower the docking affinity and the stronger the binding effect, a docking affinity below -4.25 kcal/mol indicates the presence of binding capacity between the active molecules and the target proteins, and below -5.0 kcal/mol indicates strong binding activity [44]. The top six hub targets were screened from high to low affinity, with binding energies all below -5.0 kcal/mol (Table 3), including NOS3, AKT1, EGFR, PPARA, SRC, and TNF. We can see that all targets have a strong binding ability to IPA, with NOS3 showing the strongest binding activity with a docking score of -7.3 kcal/mol (Fig. 5A-F). This suggested that IPA may improve ovarian reserve function by modulating these proteins' activity. Figure 5A as an example, IPA entered the active site of NOS3 and formed hydrophobic interactions with several residues (TRP-178, LEU-193, PHE-353, and PHE-473). In addition, IPA formed hydrogen bonds with amino acid residues TRP-356 (3.0 Å).

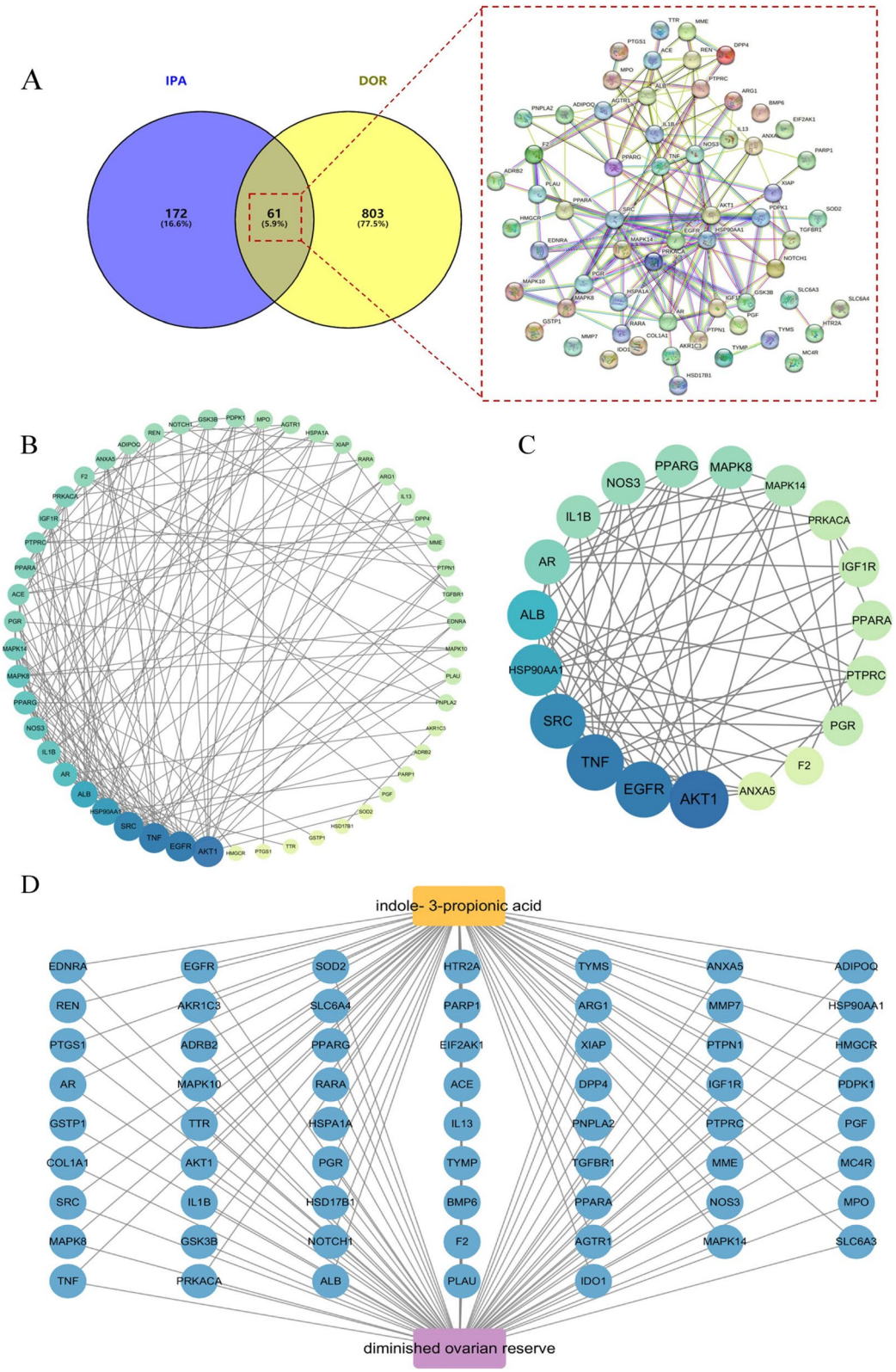

Fig. 2 Venn diagram and PPI network of potential targets. **A** Venn diagram showing the common genes between IPA and DOR. **B** PPI network of potential targets. **C** 13 hub genes of IPA against DOR were identified by network topological parameters analysis (Degree, Closeness, and Betweenness). **D** IPA-target genes-DOR network

Table 1 The hub targets information on IPA against DOR

Gene name	Gene symbol	UniProt ID
RAC-alpha serine/threonine-protein kinase	AKT1	P31749
Tumor necrosis factor	TNF	P01375
Epidermal growth factor receptor	EGFR	Q01279
Proto-oncogene tyrosine-protein kinase Src	SRC	P12931
Heat shock protein HSP 90-alpha	HSP90AA1	P30946
Albumin	ALB	P02768
Androgen receptor	AR	P10275
Nitric oxide synthase, endothelial	NOS3	P29474
Peroxisome proliferator-activated receptor gamma	PPARG	P37231
Mitogen-activated protein kinase 8	MAPK8	P45983
Peroxisome proliferator-activated receptor alpha	PPARA	Q07869
Receptor-type tyrosine-protein phosphatase C	PTPRC	P08575
Prothrombin	F2	P00734

Molecular dynamic simulation analyses

RMSD is an important indicator reflecting the stability of the complex. As shown in Fig. 6A, the protein NOS3 fluctuates smoothly in the simulation with a time of 100 ns, indicating that no conformational change has occurred, the small molecule IPA also remains stable along the simulations, and the complex gradually levels off after 40 ns, all indicating that the binding force of NOS3 and IPA is relatively stable. The RMSF reflects the flexibility of each residue in the protein, the results showed that the RMSF values of amino acid residues fluctuated less in the regions of 180–190, 310–350, and 450–470 ps (Fig. 6B). Besides, results of MM/GBSA showed that the binding free energy for IPA to NOS3 protein was -20.35 ± 0.71 kcal/mol (Table 4).

Experimental validation

IPA protected KGN cells from H_2O_2-induced damage

We assessed the effects of IPA on H_2O_2-induced OS damage in KGN cells, a cell line that maintains the physiological properties of normal ovarian granulosa cells [45]. H_2O_2 is commonly used to induce OS in vitro experiments, which is a major stimulus for cellular senescence [46]. First, we treated KGN cells for 2 h with various concentrations of H_2O_2 (100, 200, 300, 400, 500, and 600 μM). H_2O_2 reduced the cell viability in a dose-dependent manner, when the concentration was 300 μM, the cell viability was 51.2% (Fig. 7A), therefore this concentration was used for the OS model. Next, we evaluated the effect of IPA on cell cytotoxicity, KGN cells were treated with IPA in different concentrations (0.01, 0.1, 0.3, 0.5, 0.8, 1, 2, 3 mM) for 24 or 48 h, the CCK-8 assays showed that IPA did not cause obvious cytotoxicity to KGN cells at concentrations less than or equal to 0.8 mM at 24 and 48 h (Fig. 7B). To further identify the protective ability of IPA, we pretreated KGN cells with 0.01, 0.1, 0.3, 0.5, or 0.8 mM IPA for 24 h before conducting H_2O_2 treatment for 2 h, and the CCK-8 assays indicated that IPA can improve cell viability following H_2O_2 treatment, particularly at a concentration of 0.3 mM where the improvement is more pronounced (Fig. 7C), we thus selected 0.3 mM as the optimal treatment dose for subsequent experiments. In addition, as shown in Fig. 7D, KGN cells underwent morphological changes and became wrinkled and sparse after treatment with H_2O_2, whereas IPA pretreatment ameliorated cell morphology.

IPA pretreatment reduced intracellular ROS levels

To investigate the effect of IPA on OS in KGN cells, we determined the levels of intracellular ROS in each group. As shown in Fig. 8A, ROS production was significantly increased after treatment with H_2O_2, while pretreatment with IPA significantly reduced ROS generation. In Fig. 8B, the fluorescence intensity of each group was quantified using Image J software. This suggests that IPA may affect H_2O_2-induced ROS generation, thereby attenuating cell damage caused by OS.

IPA reversed the expression of target genes to alleviate H_2O_2-induced injury

According to the network pharmacological analyses, we further examined whether IPA affects the expression of NOS3, AKT1, EGFR, PPARA, SRC, and TNF in the OS model. We detected the mRNA and protein levels of these genes by RT-qPCR and WB assays, respectively. The results showed that H_2O_2 treatment inhibited the expression of SRC, EGFR, PPARA, and AKT1, whereas it increased the expression of TNF compared to the control group. However, pretreatment with 0.3 mM IPA significantly reversed the gene expression changes caused by H_2O_2 treatment (Fig. 9A-C).

IPA up-regulated the expression level of antioxidant-related proteins

The protein expression of NOX4, which mediates ROS production, was significantly upregulated in the H_2O_2-treated group, while the protein expression of antioxidase-related proteins such as SOD2, HO-1, and GPX4 was downregulated. However, pretreatment with IPA significantly reversed the changes in protein expression induced by H_2O_2 injury (Fig. 9D-E), suggesting that IPA protects from H_2O_2-induced damage by reducing oxidative stress levels.

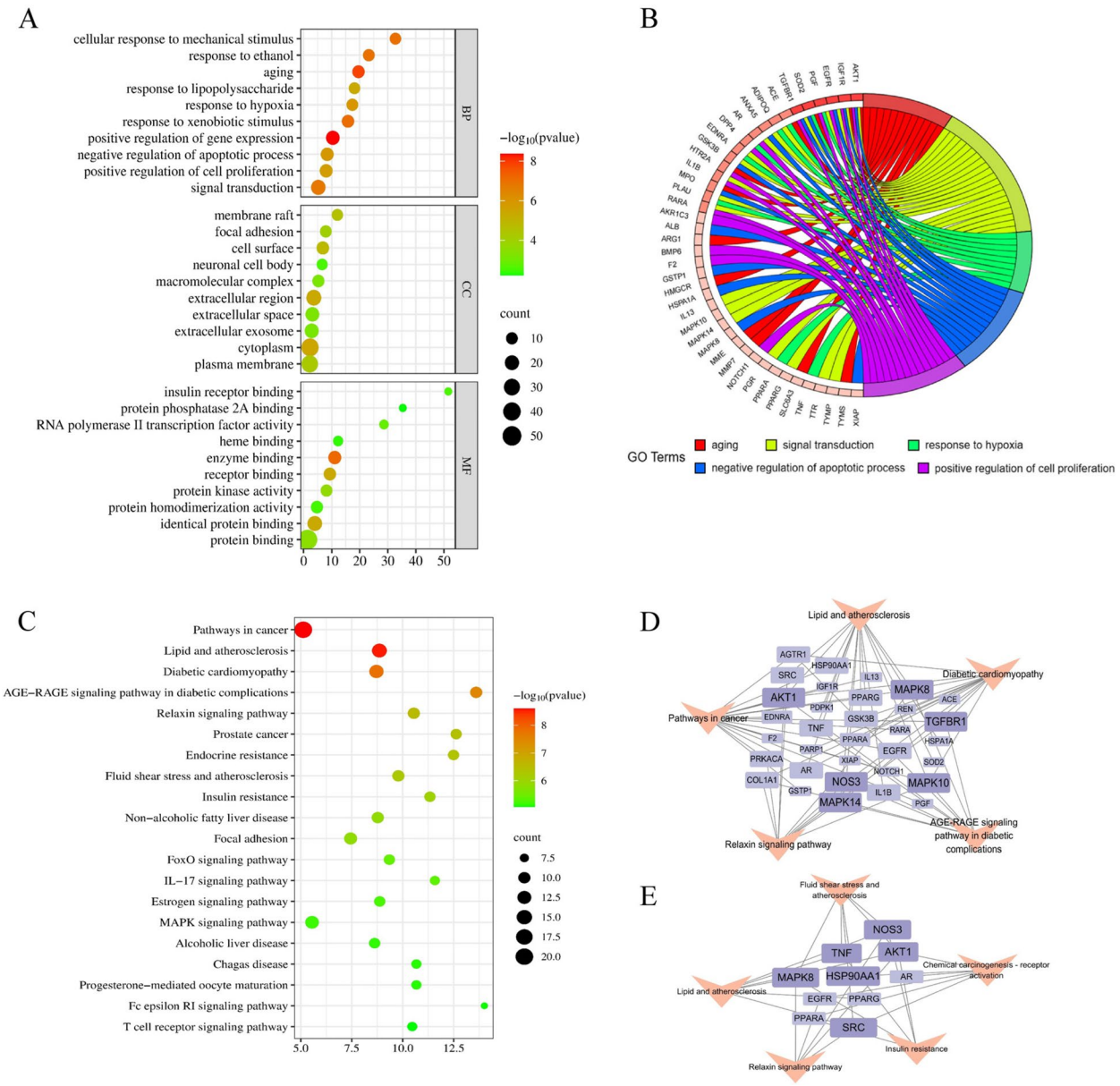

Fig. 3 The GO and KEGG enrichment analysis. **A** GO enrichment analysis (The top 10 enriched terms of each part). **B** The top 5 of the biological processes. **C** KEGG enrichment analysis of therapeutic targets (the top 20 enriched pathway). **D-E** Target-KEGG pathway network. The orange V-shaped nodes represent the pathways, and the purple square-shaped nodes represent the targets

Discussion

Diminished ovarian reserve is considered a prerequisite for POF, which seriously affects the fertility and health of women of reproductive age [1]. Studies have found that OS may be one of the important factors causing ovulation disorders and ovarian aging in women, antioxidant therapies have therefore been used clinically as an adjunct therapy to improve ovarian reserve function [3–5], and the search for new active substances with potential antioxidant properties was long pursued. As mentioned previously, IPA is recognized as a potent scavenger of free radicals and is considered to be an effective antioxidant, we therefore hypothesized that IPA is a potential compound for improving ovarian reserve function. In the present study, for the first time, we explored the possible molecular mechanism of IPA in the treatment of DOR using network pharmacology and in vitro experiments. Based on PPI network analysis, we identified six core genes with the highest degree of interaction: NOS3, AKT1, EGFR, PPARA, SRC, and TNF, moreover, these

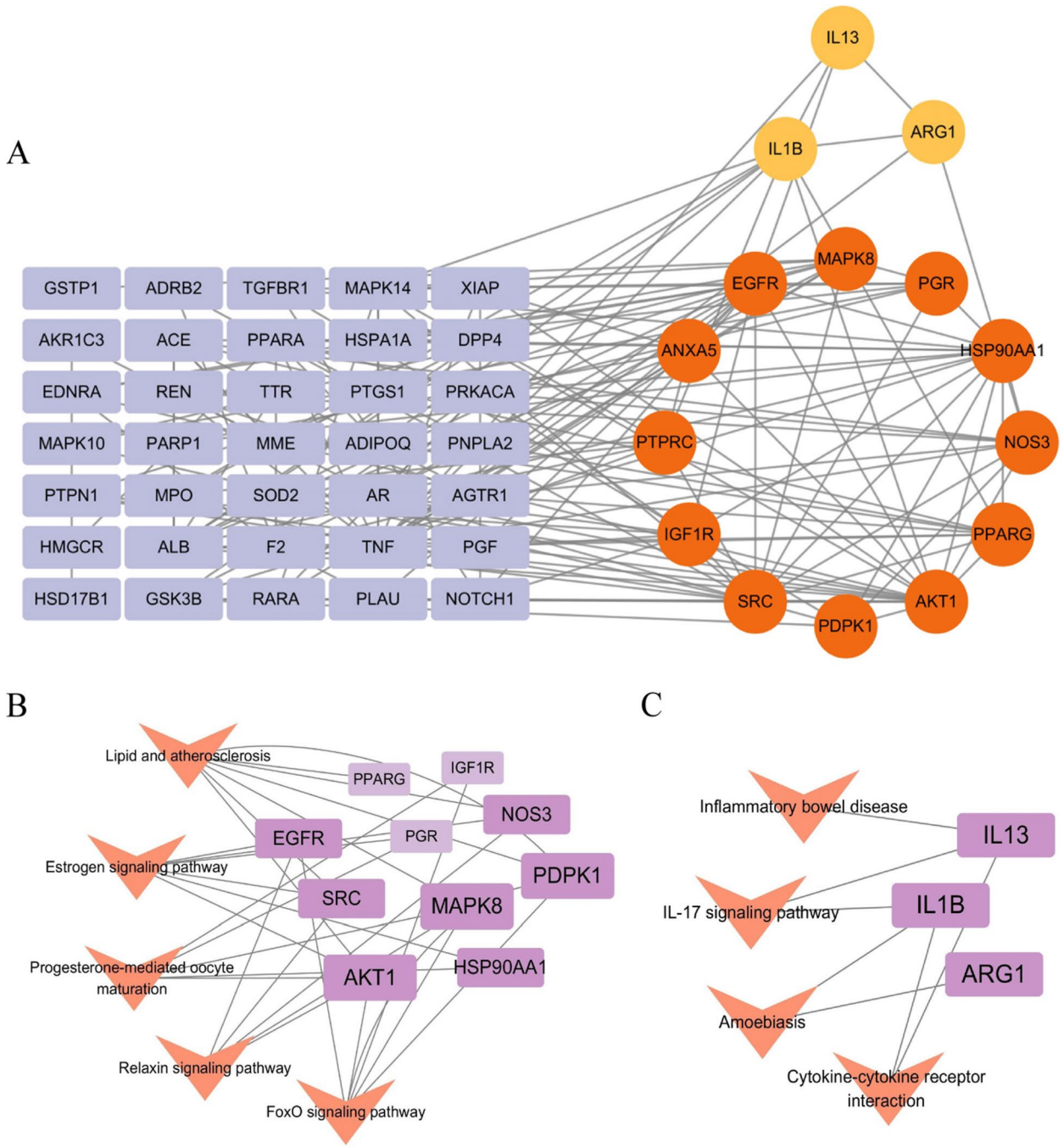

Fig. 4 **A** Function modules-based network analysis. Cluster1 in red, and Cluster2 in yellow. The purple squares represent non clustering genes. **B-C** Target-KEGG pathway network. The orange V-shaped nodes represent the pathways, and the purple square-shaped nodes represent the targets

hub targets exhibited good affinity for molecular docking with IPA and could be key targets for treating DOR.

IPA's six core genes in DOR

Nitric oxide synthases (NOS) can catalyze the conversion of L-arginine to L-citrulline with the production of nitric oxide (NO) [47], which is generally considered to be required for the preovulatory cascade [48]. Two isoforms in NOS, Inducible NOS (iNOS) and endothelial NOS (eNOS, also known as NOS3) have been well-confirmed to exist in the ovarian follicles [49]. NOS3 is thought to be associated with ovulation-related

Table 2 KEGG pathways of the two MCODE modules

MCODE	Pathway	Genes count	*P*-value
Cluster-1	Lipid and atherosclerosis	7	5.81E-08
Cluster-1	Estrogen signaling pathway	6	2.95E-07
Cluster-1	Progesterone-mediated oocyte maturation	5	4.46E-06
Cluster-1	Relaxin signaling pathway	5	1.14E-05
Cluster-1	FoxO signaling pathway	5	1.21E-05
Cluster-2	Inflammatory bowel disease	2	0.015
Cluster-2	IL-17 signaling pathway	2	0.023
Cluster-2	Amoebiasis	2	0.027
Cluster-2	Cytokine-cytokine receptor interaction	2	0.071

Table 3 The molecular docking parameters and results

Serial number	Targets	PDB ID	Box_center (x, y, z)/Å	Affinity/(kcal/mol)
1	NOS3	6AV7	83.5, -0.9, -190.0	-7.3
2	AKT1	3O96	6.3, -8.0, 17.3	-6.0
3	EGFR	6XL4	-1.8, 13.5, -25.0	-5.9
4	PPARA	6KAY	5.4, 2.0, 2.1	-5.8
5	SRC	4K11	21.2, 33.8, 67.2	-5.5
6	TNF	5M2M	0.6, 22.4, 23.1	-5.2

hemodynamic changes, and genetic deletion of NOS3 may interfere with the local blood supply of the ovary, thereby damaging follicle recruitment and ovulation [50]. Hefler et al. found that NOS3-deficient mice have a lower ovulation rate [51]. Interestingly, Pulakazhi et al. reported that IPA supplementation reduced NOS3 protein expression in aortic tissues in mice, which could normalize the abnormal vasodilatory response [52]. A recent study also found that the antioxidant effect of IPA reversed NO levels in the ovary and uterus of rats that were damaged by epirubicin [53].

As a serine/threonine protein kinase, AKT is widely expressed in human ovaries, including oocytes, granulosa cells (GCs), and follicles at all stages of growth [54]. AKT1 is involved in many physiological processes, including the activation of primordial follicles, the proliferation, and differentiation of GCs [55]. It has been reported that AKT1-/- female mice have reduced fertility, as evidenced by disrupted estrous cycles and reduced numbers of antral follicles [56]. There is currently no literature reporting a direct relationship between IPA and AKT. Notably, IPA has a similar chemical structure to melatonin, and IPA has been reported to outperform melatonin in its ability to scavenge hydroxyl radicals in kinetic competition experiments [10]. Recent studies have shown that melatonin inhibits granulosa cell autophagy and slows follicular atresia by activating the PI3K/Akt/mTOR pathway, thereby protecting ovarian function [57, 58]. Guo et al. found that melatonin can inhibit palmitic acid-induced insulin resistance and apoptosis in human granulosa cell lines through activation of the PI3K/AKT pathway [59]. Therefore, it is reasonable to speculate that IPA may improve ovarian function by modulating AKT levels.

Tumor necrosis factor (TNF), formerly known as TNF-α, is one of the key cytokines that involve and maintain inflammatory responses. Abnormally elevated levels of proinflammatory cytokines such as IL-6 and TNF-α play an essential role in ovarian aging [60]. It has been reported that TNF-α levels in follicular fluid were significantly higher than those in serum in patients with premature ovarian insufficiency [61]. Additionally, an animal study showed that TNF-α levels in the serum and ovaries of POF mice were increased compared to controls [62]. The anti-inflammatory properties of IPA have been demonstrated in vitro and in vivo experiments. Recently, a study found that indole supplementation reduced TNF-α and IL-6 levels in the brains of Alzheimer's disease mice, thereby reducing their neuroinflammatory response [14]. Similarly, Garcez et al. reported that pretreatment with IPA prevented LPS-induced increases in the levels of

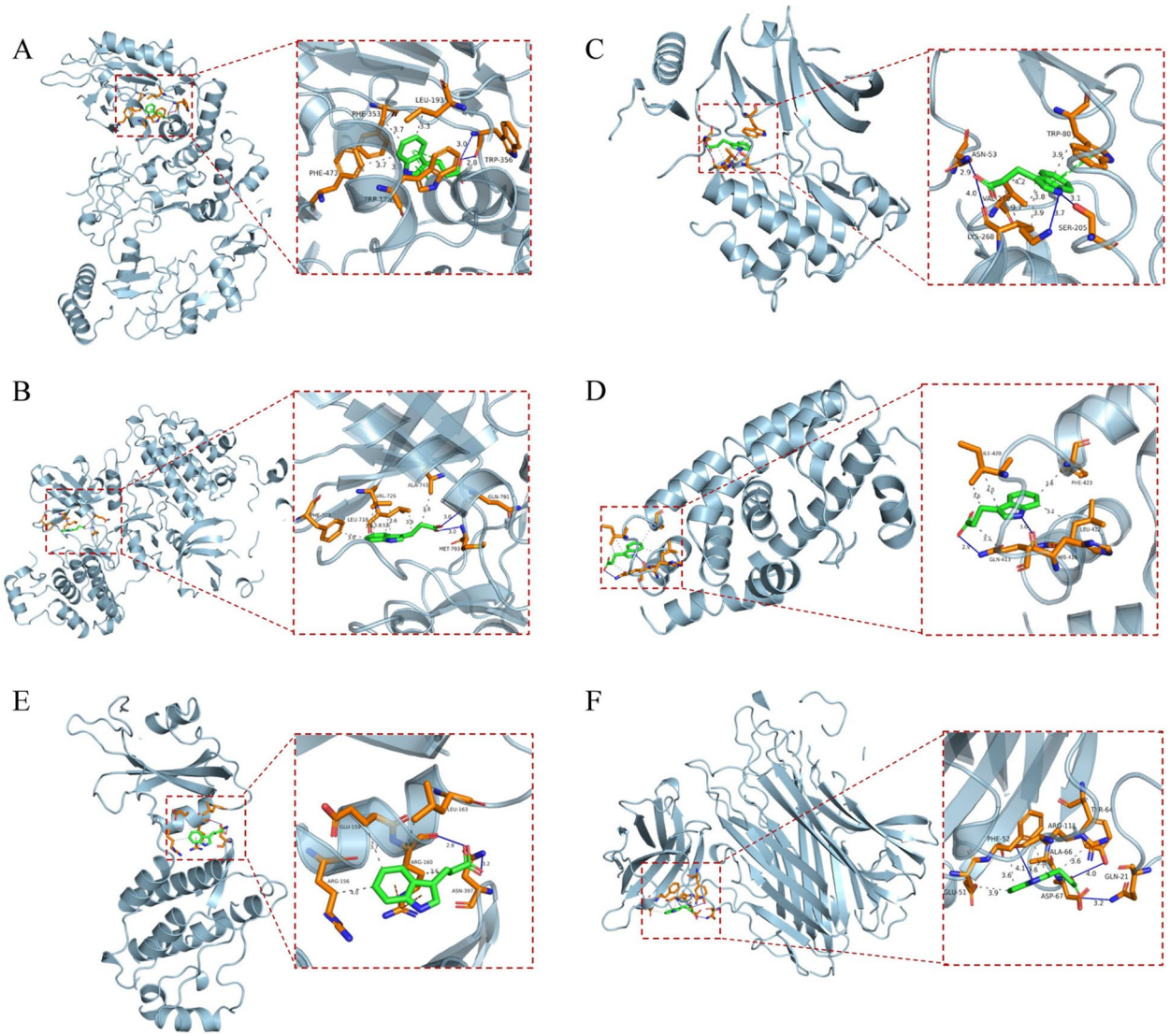

Fig. 5 Molecular docking of the top six hub targets with IPA. **A** The binding poses of NOS3 complexed with IPA. **B** The binding poses of AKT1 complexed with IPA. **C** The binding poses of EGFR complexed with IPA. **D** The binding poses of PPARA complexed with IPA. **E** The binding poses of SRC complexed with IPA. **F** The binding poses of TNF complexed with IPA

inflammatory factors such as TNF-α [63]. Furthermore, Owumi and colleagues also preliminarily demonstrated the anti-inflammatory activity of IPA in rat ovary and uterus [53].

EGFR is a transmembrane receptor tyrosine kinase, it affects the proliferation and apoptosis of ovarian GCs and induces the division and maturation of oocytes [64]. EGFR can activate several downstream signaling pathways, such as JAK/STAT, PI3K/AKT, and MAPK/ERK, which play an important role in oocyte maturation, cumulus expansion, and ovulation [65–67]. In addition, it has been shown that in patients with polycystic ovary syndrome, EGFR was significantly downregulated in germinal vesicle (GV) stage oocytes, which in turn caused more production of immature follicles [68]. There is an important role for PPARs in regulating glucose, lipid metabolism, and inflammatory processes, as well as in various cell differentiation, proliferation, and apoptosis processes. Furthermore, PPARα is mainly expressed in the theca and stromal cells of the rat ovary [69]. SRC is a non-receptor tyrosine kinase encoded that is activated by many extracellular signaling molecules [70]. Estrogen runs through the whole process of follicle recruitment,

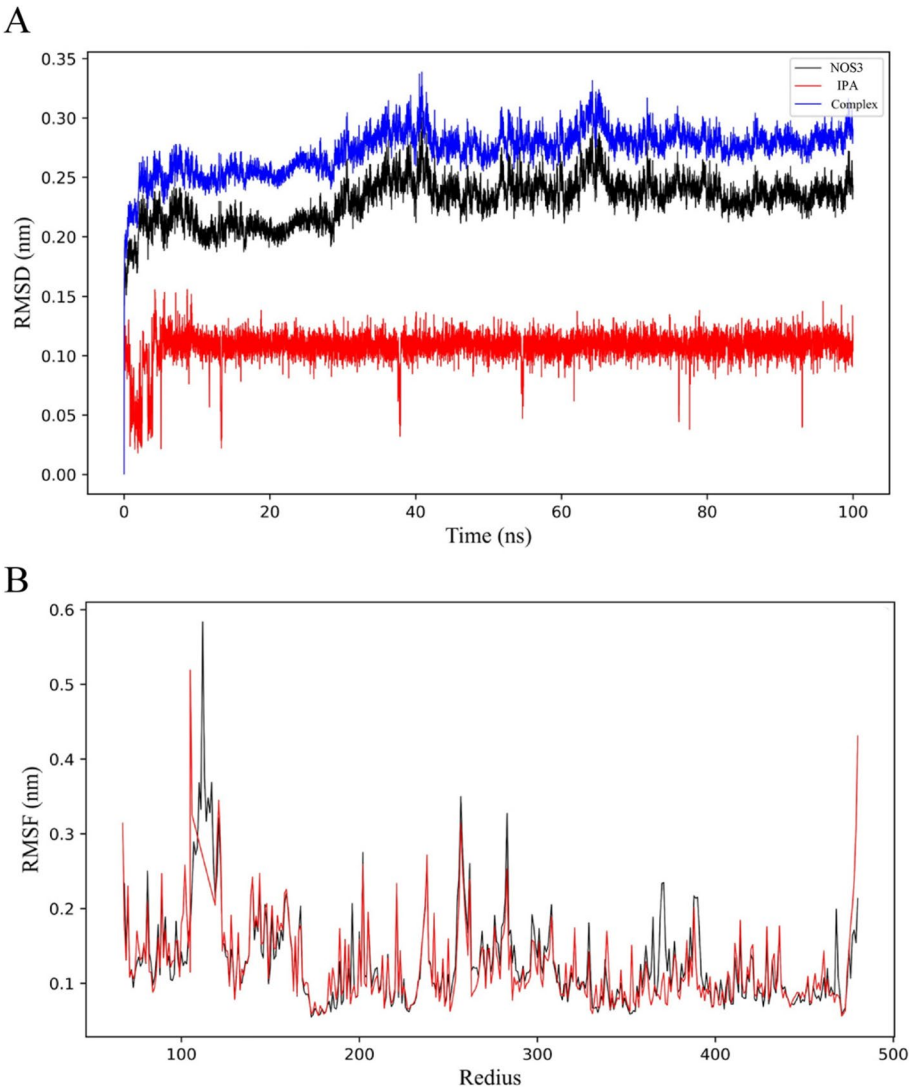

Fig. 6 Molecular dynamics simulation between IPA and NOS3 protein. **A** RMSD. **B** RMSF

Table 4 Binding free energy calculations by MM/GBSA (kcal/mol)

Energy	NOS3-indole-3-propionic acid
VDWAALS	-26.19 ± 0.10
ΔE_{EL}	-9.42 ± 0.60
ΔE_{GB}	18.57 ± 0.36
ΔE_{SURF}	-3.31 ± 0.10
ΔG_{gas}	-35.61 ± 0.61
ΔG_{solv}	15.26 ± 0.36
ΔG_{MMGBSA}	-20.35 ± 0.71

VDWAALS Van der Waals energy, ΔE_{EL} Electrostatic energy, ΔE_{GB} Polar solvation energy, ΔE_{SURF} Non polar solvation energy, ΔG_{gas} Molecular mechanics term energy, ΔG_{solv} Solvation energy, ΔG_{MMGBSA} Binding free energy

selection, and dominance. As a downstream protein of the estrogen receptor ESR1, SRC is an important mediator of estrogen signaling and its biological role [71]. Although the multiple biological effects on the human health of IPA have been widely revealed, there are currently fewer studies of IPA in the female reproductive system, and no basic studies have directly reported that IPA can improve ovarian reserve function through the six hub targets mentioned above. However, the molecular docking results of this study confirmed that all six targets have a good binding ability to IPA, and the molecular dynamics simulations further demonstrated the binding stability of NOS3 and IPA. Moreover, in vitro experiments showed that IPA reversed the mRNA and protein expression of these six targets

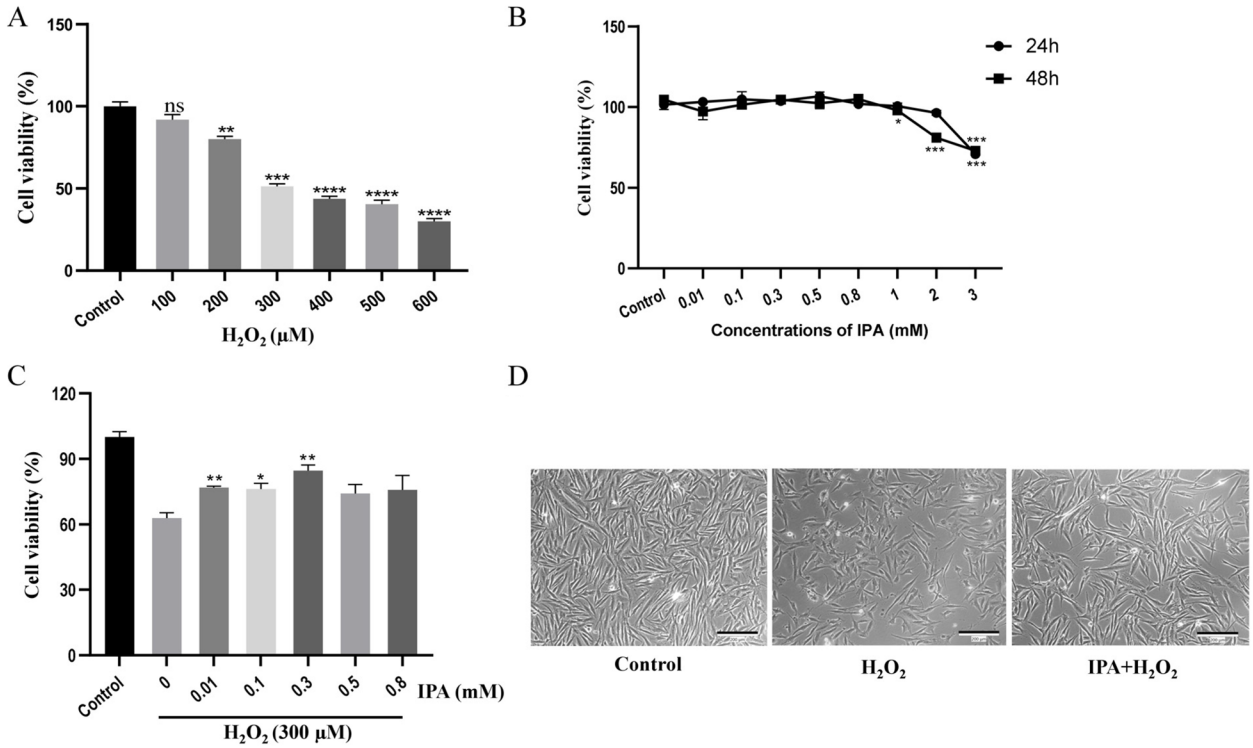

Fig. 7 **A** Cell activity of KGN cell lines treated with H_2O_2 for 2 h. $^{**}P < 0.01$, $^{***}P < 0.001$ vs. the control group. **B** Cell activity of KGN cell lines treated with IPA for 24 and 48 h. $^{*}P < 0.05$, $^{***}P < 0.001$ vs. the control group. **C** KGN cell lines were pretreated with indicated concentrations of IPA for 24 h, followed by H_2O_2 for 2 h. Cell viability was determined by CCK-8. $^{*}P < 0.05$, $^{**}P < 0.01$ vs. the non-IPA group. **D** The changes in cell morphology after H_2O_2 administration with or without pretreatment with IPA at a concentration of 0.3 mM (200×). The results were expressed as the average of three independent experiments

in KGN cells, and in combination with their biological functions and physiological roles in the ovary, we hypothesized that IPA may exert a beneficial effect in ovaries by regulating these targets. Overall, the above-mentioned targets provide a basis for further exploring the molecular mechanisms of IPA in treating DOR.

Biological processes and pathways by which IPA functions

Based on PPI analysis and the CentiScaPe module of the Cytoscape, we obtained 61 potential targets and 13 hub genes, then performed GO enrichment and KEGG pathway analysis on them. These potential therapeutic targets are mainly involved in aging, signal transduction, response to hypoxia, negative regulation of apoptotic process, and positive regulation of cell proliferation. IPA has been confirmed to play a beneficial role in aging and some age-related diseases such as Alzheimer's disease and multiple sclerosis [14, 72]. Notably, our previous study also found that IPA levels in follicular fluid were significantly lower in ovarian aging patients [22]. Furthermore, the AGE-RAGE signaling pathway and relaxin signaling pathway were the two most enriched pathways of IPA against DOR. Advanced glycation end products (AGEs) have been reported to be associated with ovarian aging [73]. On the one hand, glycosylation can cause irreversible protein damage, which will transform a normally structured protein into an abnormally aged one [74]. On the other hand, AGEs and their receptor RAGE interactions induce inflammation and oxidative stress [75], which has been shown to play key roles in poor ovarian reserve function. Relaxin can modulate various cytokines and signal pathways such as PI3K/AKT or ERK to exert anti-inflammatory and anti-fibrotic effects. It has been reported that impaired relaxin signaling may be linked to smaller ovaries and uterus in the offspring of female mice [76]. Additionally, Feugang et al. found that the relaxin receptor named RXFP1 mRNA and its protein are expressed on both granulosa cells and oocytes of porcine sinus follicles, suggesting that relaxin can promote oocyte maturation [77].

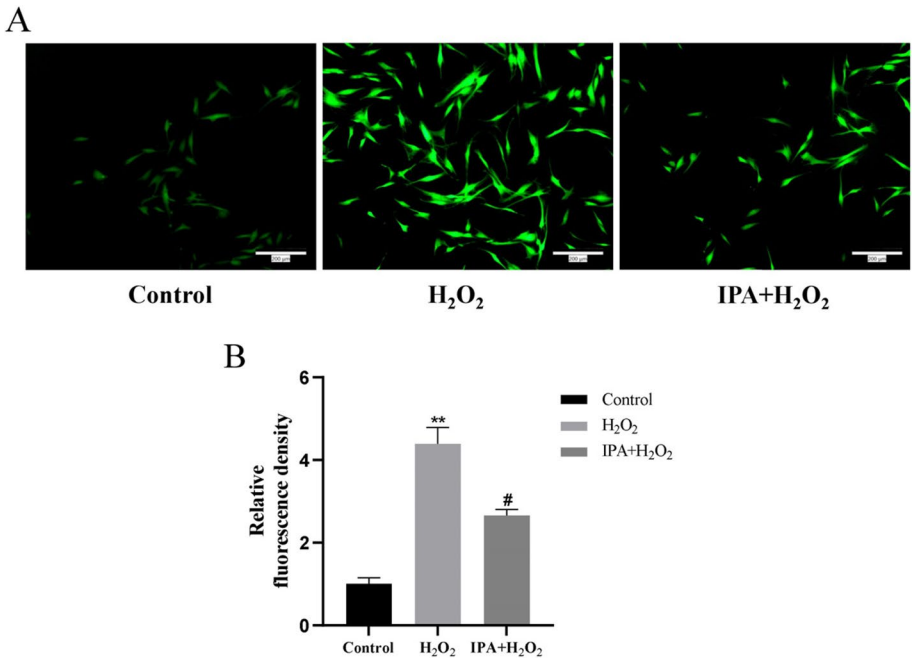

Fig. 8 **A** The level of reactive oxygen species (ROS) was detected using ROS assay kit. **B** Quantification of the ROS level in each group. $^{*}P < 0.05$ vs. the control group. The results were expressed as the average of three independent experiments. $^{\#}P < 0.05$ vs. the H_2O_2 group. The results were expressed as the average of three independent experiments

To further explore IPA mechanisms in improving ovarian function, we used the MCODE plugin to divide the entire network target into 2 tightly connected core modules, and functional enrichment analyses were carried out on these modules, as shown in Fig. 4B-C. The first module contains estrogen signaling pathway, progesterone-mediated oocyte maturation, and related signaling pathway. Estrogen signaling pathway is crucial to maintaining normal female reproductive endocrine function [78]. Interestingly, recent work by Owumi et al. found that IPA prevented epirubicin-induced decreases in serum estradiol and follicle-stimulating hormone levels in female rats, thereby maintaining serum hormone stability [53]. The second module is related to inflammatory signaling pathways. These modules reflect the effects of IPA on hormonal and endocrine regulation, anti-inflammation, and oocyte maturation.

IPA alleviates cellular damage and oxidative stress

As already stated, OS is one of the important factors leading to DOR. IPA is considered an essential ROS scavenger that protects cells from OS damage. Gundu et al. found that IPA attenuated high glucose-induced endoplasmic reticulum stress and mitochondrial dysfunction in neuronal cells [79]. Moreover, IPA was found to significantly reduce the lipid peroxidation damage caused by potassium iodate in porcine thyroid [8]. In the present study, our in vitro experiments showed that IPA pretreatment improved cell viability and attenuated H_2O_2-induced intracellular ROS production. In addition, we also discovered the protein expressions of SOD2, HO-1, and GPX4 in KGN cells were down-regulated after H_2O_2 treatment, and could be reversed by IPA pretreatment. These results suggest that IPA may protect KGN cells from H_2O_2-induced damage. However, this in vitro experiment has some limitations as the role of IPA was only preliminarily verified in the KGN cell line. In future studies, firstly, the above results need to be validated in normal granulosa cell lines. Secondly, the effect of IPA intervention on ovarian reserve function needs to be further clarified by extracting and culturing primary granulosa cells from clinical patients, as well as by establishing animal experimental models.

Conclusion

This work demonstrates that several targets, including NOS3, AKT1, EGFR, PPARA, SRC, and TNF, as well as biological processes, including aging, signal transduction, response to hypoxia, negative regulation of

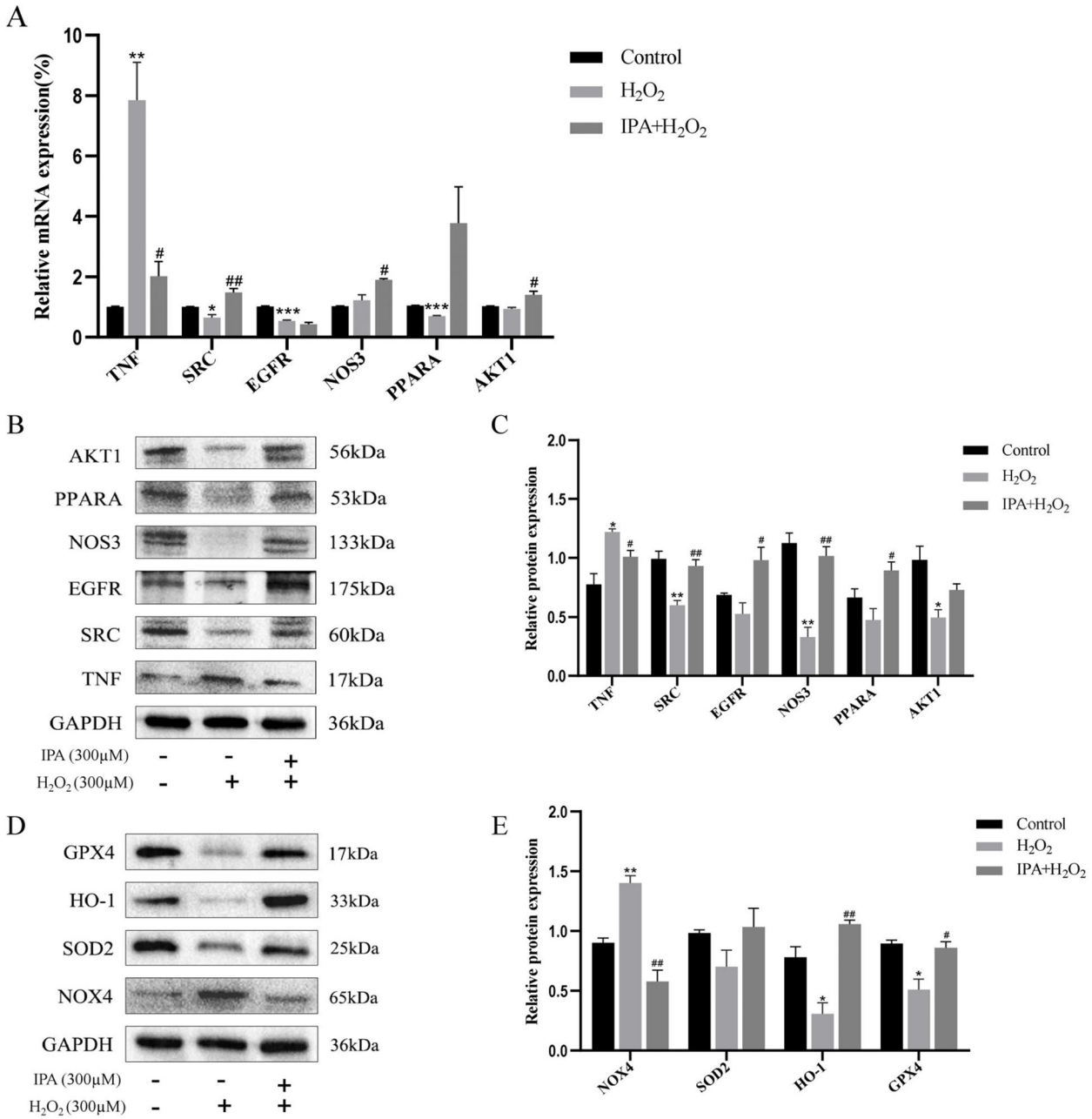

Fig. 9 **A** mRNA expression of NOS3, AKT1, EGFR, PPARA, SRC, and TNF in KGN cells. **B-C** Expression of TNF, SRC, EGFR, NOS3, PPARA, and AKT1 proteins in KGN cells. **D-E** Protein expression of oxidative stress and antioxidant-related proteins NOX4, SOD2, HO-1, and GPX4. $^{*}P < 0.05$, $^{**}P < 0.01$, $^{***}P < 0.001$ vs. the control group. $^{\#}P < 0.05$, $^{\#\#}P < 0.01$ vs. the H_2O_2 group. The results were expressed as the average of three independent experiments

apoptotic process, and positive regulation of cell proliferation, and signaling pathways, such as AGE-RAGE and relaxin signaling pathway, are involved in the mechanism of IPA against DOR. Our results provide new insights for better improvement of ovarian reserve function in the clinic. However, the current findings are mainly based on network pharmacology and preliminary in vitro experiments, and further in vivo and clinical research are required to confirm the mechanisms revealed by our study.

Supplementary Information

The online version contains supplementary material available at https://doi.org/10.1186/s12906-024-04611-1.

Supplementary Material 1.
Supplementary Material 2.
Supplementary Material 3.
Supplementary Material 4.
Supplementary Material 5.
Supplementary Material 6.
Supplementary Material 7.

Acknowledgements
Not applicable.

Authors' contributions
AHL, ZJL, and HFS: data analysis, write the original manuscript and preliminary revision. AHL and ZJL: data collation, methodology and visualization. HFS and WJD: software and experimental validation. YBJ and LYW: literature collection and validation. RZ: language editing/appropriateness. XHZ and PPJ: design the project, responsible for integrity of study, and critically revised the manuscript. XHZ is the main corresponding author. All the authors provided a critical review and approved the final submission.

Funding
This study was supported by grants from the National Natural Science Foundation of China (81960273); Lanzhou Youth Science and Technology Talent Innovation Project (2023–4-47); Lanzhou Chengguan District Science and Technology Plan Project (2023–11-3); Natural Science Foundation of Gansu Province (23JRRA1603); and Hospital Fund of the First Hospital of Lanzhou University (ldyyyn2022-20).

Availability of data and materials
All data generated or analyzed during this study are included in this published article and its supplementary information files.

Declarations

Ethics approval and consent to participate
Not applicable.

Consent for publication
Not applicable.

Competing interests
The authors declare no competing interests.

Author details
[1]The First School of Clinical Medicine, Lanzhou University, Lanzhou, Gansu, China. [2]Reproductive Medicine Center, The First Hospital of Lanzhou University, Chengguan District, No. 1 Dong Gang Xi Road, Lanzhou, Gansu 730000, China. [3]Key Laboratory for Reproductive Medicine and Embryo, Lanzhou, Gansu, China. [4]The Affiliated Hospital of Gansu University of Chinese Medicine, Lanzhou, Gansu, China.

Received: 31 May 2023 Accepted: 13 August 2024
Published online: 27 August 2024

References

1. Pfister A, Crawford NM, Steiner AZ. Association between diminished ovarian reserve and luteal phase deficiency. Fertil Steril. 2019;112(2):378–86. https://doi.org/10.1016/j.fertnstert.2019.03.032.
2. Cedars MI. Managing poor ovarian response in the patient with diminished ovarian reserve. Fertil Steril. 2022;117(4):655–6.
3. Liu X, Lin X, Mi Y, Li J, Zhang C. Grape Seed Proanthocyanidin Extract Prevents Ovarian Aging by Inhibiting Oxidative Stress in the Hens. Oxid Med Cell Longev. 2018;2018:9390810. https://doi.org/10.1155/2018/9390810.
4. Bai L, He G, Gao C, et al. Tanshinone IIA enhances the ovarian reserve and attenuates ovarian oxidative stress in aged mice. Vet Med Sci. 2022;8(4):1617–25. https://doi.org/10.1002/vms3.811.
5. Adeniyi JN, Nlooto M, Ngcobo M, Moodley R, Gomo E. Phytochemical profile and in vitro antioxidant activity of Emelia M (EMB), Mshikazi and Delosma H herbal medicines as demonstrated in THP-1 and Jurkat leukaemia cell lines. Afr Health Sci. 2021;21(4):1924–37. https://doi.org/10.4314/ahs.v21i4.51.
6. van der Goot AT, Nollen EA. Tryptophan metabolism: entering the field of aging and age-related pathologies. Trends Mol Med. 2013;19(6):336–44. https://doi.org/10.1016/j.molmed.2013.02.007.
7. Wang S, Feng R, Chen GJ, et al. Simultaneous determination of serum tryptophan metabolites in an older Chinese population. Biomed Chromatogr. 2023;37(1): e5512. https://doi.org/10.1002/bmc.5512.
8. Mokhtari F, Akbari Asbagh F, Azmoodeh O, Bakhtiyari M, Almasi-Hashiani A. Effects of Melatonin Administration on Chemical Pregnancy Rates of Polycystic Ovary Syndrome Patients Undergoing Intrauterine Insemination: A Randomized Clinical Trial. Int J Fertil Steril. 2019;13(3):225–9. https://doi.org/10.22074/ijfs.2019.5717.
9. Cosme P, Rodríguez AB, Garrido M, Espino J. Coping with Oxidative Stress in Reproductive Pathophysiology and Assisted Reproduction: Melatonin as an Emerging Therapeutical Tool. Antioxidants (Basel). 2022;12(1):86. https://doi.org/10.3390/antiox12010086.
10. Karbownik M, Stasiak M, Zygmunt A, et al. Protective effects of melatonin and indole-3-propionic acid against lipid peroxidation, caused by potassium bromate in the rat kidney. Cell Biochem Funct. 2006;24(6):483–9.
11. Chyan YJ, Poeggeler B, Omar RA, et al. Potent neuroprotective properties against the Alzheimer beta-amyloid by an endogenous melatonin-related indole structure, indole-3-propionic acid. J Biol Chem. 1999;274(31):21937–42.
12. Rynkowska A, Stępniak J, Karbownik-Lewińska M. Melatonin and Indole-3-Propionic Acid Reduce Oxidative Damage to Membrane Lipids Induced by High Iron Concentrations in Porcine Skin. Membranes (Basel). 2021;11(8):571.
13. Hwang IK, Yoo KY, Li H, et al. Indole-3-propionic acid attenuates neuronal damage and oxidative stress in the ischemic hippocampus. J Neurosci Res. 2009;87(9):2126–37.
14. Sun J, Zhang Y, Kong Y, et al. Microbiota-derived metabolite Indoles induced aryl hydrocarbon receptor activation and inhibited neuroinflammation in APP/PS1 mice. Brain Behav Immun. 2022;106:76–88.
15. Tuomainen M, Lindström J, Lehtonen M, et al. Associations of serum indolepropionic acid, a gut microbiota metabolite, with type 2 diabetes and low-grade inflammation in high-risk individuals. Nutr Diabetes. 2018;8(1):35.
16. Sehgal R, Ilha M, Vaittinen M, et al. Indole-3-Propionic Acid, a Gut-Derived Tryptophan Metabolite, Associates with Hepatic Fibrosis. Nutrients. 2021;13(10):3509.
17. Alexeev EE, Lanis JM, Kao DJ, et al. Microbiota-Derived Indole Metabolites Promote Human and Murine Intestinal Homeostasis through Regulation of Interleukin-10 Receptor. Am J Pathol. 2018;188(5):1183–94.
18. Jennis M, Cavanaugh CR, Leo GC, et al. Microbiota-derived tryptophan indoles increase after gastric bypass surgery and reduce intestinal permeability in vitro and in vivo. Neurogastroenterol Motil. 2018;30(2):https://doi.org/10.1111/nmo.13178.
19. Konopelski P, Mogilnicka I. Biological Effects of Indole-3-Propionic Acid, a Gut Microbiota-Derived Metabolite, and Its Precursor Tryptophan in Mammals' Health and Disease. Int J Mol Sci. 2022;23(3):1222.
20. Karbownik M, Stasiak M, Zasada K, et al. Comparison of potential protective effects of melatonin, indole-3-propionic acid, and propylthiouracil against lipid peroxidation caused by potassium bromate in the thyroid gland. J Cell Biochem. 2005;95(1):131–8.
21. Negatu DA, Gengenbacher M, Dartois V, et al. Indole Propionic Acid, an Unusual Antibiotic Produced by the Gut Microbiota, With Anti-inflammatory and Antioxidant Properties. Front Microbiol. 2020;11: 575586.

22. Liu A, Shen H, Li Q, et al. Determination of tryptophan and its indole metabolites in follicular fluid of women with diminished ovarian reserve. Sci Rep. 2023;13(1):17124. https://doi.org/10.1038/s41598-023-44335-9.
23. Ruebel ML, Piccolo BD, Mercer KE, et al. Obesity leads to distinct metabolomic signatures in follicular fluid of women undergoing in vitro fertilization. Am J Physiol Endocrinol Metab. 2019;316(3):E383–96.
24. Yang L, Xu H, Chen Y, et al. Melatonin: Multi-Target Mechanism Against Diminished Ovarian Reserve Based on Network Pharmacology. Front Endocrinol (Lausanne). 2021;12: 630504. https://doi.org/10.3389/fendo.2021.630504.
25. Yan H, Li Y, Yang B, et al. Exploring the mechanism of action of Yiyi Fuzi Baijiang powder in colorectal cancer based on network pharmacology and molecular docking studies. Biotechnol Genet Eng Rev. Published online February 3, 2023. https://doi.org/10.1080/02648725.2023.2167765.
26. Kim S, Thiessen PA, Bolton EE, et al. PubChem Substance and Compound databases. Nucleic Acids Res. 2016;44(D1):D1202–13.
27. Daina A, Michielin O, Zoete V. SwissTargetPrediction: updated data and new features for efficient prediction of protein targets of small molecules. Nucleic Acids Res. 2019;47(W1):W357–64.
28. Yao ZJ, Dong J, Che YJ, et al. TargetNet: a web service for predicting potential drug-target interaction profiling via multi-target SAR models. J Comput Aided Mol Des. 2016;30(5):413–24.
29. Liu Z, Guo F, Wang Y, et al. BATMAN-TCM: a Bioinformatics Analysis Tool for Molecular mechANism of Traditional Chinese Medicine. Sci Rep. 2016;6:21146.
30. Wang X, Shen Y, Wang S, et al. PharmMapper 2017 update: a web server for potential drug target identification with a comprehensive target pharmacophore database. Nucleic Acids Res. 2017;45(W1):W356–60.
31. UniProt Consortium. UniProt: the Universal Protein Knowledgebase in 2023. Nucleic Acids Res. 2023;51(D1):D523–31.
32. Amberger JS, Bocchini CA, Schiettecatte F, et al. OMIM.org: Online Mendelian Inheritance in Man (OMIM®), an online catalog of human genes and genetic disorders. Nucleic Acids Res. 2015;43(Database issue):D789–D798.
33. Safran M, Dalah I, Alexander J, et al. GeneCards Version 3: the human gene integrator. Database (Oxford). 2010;2010:baq020.
34. Wishart DS, Feunang YD, Guo AC, et al. DrugBank 5.0: a major update to the DrugBank database for 2018. Nucleic Acids Res. 2018;46(D1):D1074–D1082.
35. Piñero J, Ramírez-Anguita JM, Saüch-Pitarch J, et al. The DisGeNET knowledge platform for disease genomics: 2019 update. Nucleic Acids Res. 2020;48(D1):D845–55.
36. Szklarczyk D, Franceschini A, Wyder S, et al. STRING v10: protein-protein interaction networks, integrated over the tree of life. Nucleic Acids Res. 2015;43(Database issue):D447–D452.
37. Sherman BT, Hao M, Qiu J, et al. DAVID: a web server for functional enrichment analysis and functional annotation of gene lists (2021 update). Nucleic Acids Res. 2022;50(W1):W216–21.
38. Ito K, Murphy D. Application of ggplot2 to Pharmacometric Graphics. CPT Pharmacometrics Syst Pharmacol. 2013;2(10): e79.
39. Kohl M, Wiese S, Warscheid B. Cytoscape: software for visualization and analysis of biological networks. Methods Mol Biol. 2011;696:291–303. https://doi.org/10.1007/978-1-60761-987-1_18.
40. Morris GM, Huey R, Lindstrom W, et al. AutoDock4 and AutoDockTools4: Automated docking with selective receptor flexibility. J Comput Chem. 2009;30(16):2785–91.
41. Trott O, Olson AJ. AutoDock Vina: improving the speed and accuracy of docking with a new scoring function, efficient optimization, and multithreading. J Comput Chem. 2010;31(2):455–61.
42. Pronk S, Páll S, Schulz R, et al. GROMACS 4.5: a high-throughput and highly parallel open source molecular simulation toolkit. Bioinformatics. 2013;29(7):845–854. https://doi.org/10.1093/bioinformatics/btt055.
43. Chen Y, Zheng Y, Fong P, Mao S, Wang Q. The application of the MM/GBSA method in the binding pose prediction of FGFR inhibitors. Phys Chem Chem Phys. 2020;22(17):9656–63. https://doi.org/10.1039/d0cp00831a.
44. Hsin KY, Ghosh S, Kitano H. Combining machine learning systems and multiple docking simulation packages to improve docking prediction reliability for network pharmacology. PLoS ONE. 2013;8(12): e83922. https://doi.org/10.1371/journal.pone.0083922.
45. Havelock JC, Rainey WE, Carr BR. Ovarian granulosa cell lines. Mol Cell Endocrinol. 2004;228(1–2):67–78. https://doi.org/10.1016/j.mce.2004.04.018.
46. Mahajan AS, Arikatla VS, Thyagarajan A, et al. Creatine and Nicotinamide Prevent Oxidant-Induced Senescence in Human Fibroblasts. Nutrients. 2021;13(11):4102. Published 2021 Nov 16. https://doi.org/10.3390/nu13114102.
47. Pircher A, Treps L, Bodrug N, et al. Endothelial cell metabolism: A novel player in atherosclerosis? Basic principles and therapeutic opportunities Atherosclerosis. 2016;253:247–57.
48. Zamberlam G, Sahmi F, Price CA. Nitric oxide synthase activity is critical for the preovulatory epidermal growth factor-like cascade induced by luteinizing hormone in bovine granulosa cells. Free Radic Biol Med. 2014;74:237–44.
49. Zamberlam G, Portela V, de Oliveira JF, et al. Regulation of inducible nitric oxide synthase expression in bovine ovarian granulosa cells. Mol Cell Endocrinol. 2011;335(2):189–94.
50. Shukovski L, Tsafriri A. The involvement of nitric oxide in the ovulatory process in the rat. Endocrinology. 1994;135(5):2287–90.
51. Hefler LA, Gregg AR. Inducible and endothelial nitric oxide synthase: genetic background affects ovulation in mice. Fertil Steril. 2002;77(1):147–51.
52. Pulakazhi Venu VK, Saifeddine M, Mihara K, et al. The pregnane X receptor and its microbiota-derived ligand indole 3-propionic acid regulate endothelium-dependent vasodilation. Am J Physiol Endocrinol Metab. 2019;317(2):E350–61.
53. Owumi SE, Adebisi GE, Odunola OA. Epirubicin toxicity in rat's ovary and uterus: A protective role of 3-Indolepropionic acid supplementation. Chem Biol Interact. 2023;374: 110414. https://doi.org/10.1016/j.cbi.2023.110414.
54. Goto M, Iwase A, Ando H, et al. PTEN and Akt expression during growth of human ovarian follicles. J Assist Reprod Genet. 2007;24(11):541–6.
55. Cecconi S, Mauro A, Cellini V, et al. The role of Akt signalling in the mammalian ovary. Int J Dev Biol. 2012;56(10–12):809–17.
56. Brown C, LaRocca J, Pietruska J, et al. Subfertility caused by altered follicular development and oocyte growth in female mice lacking PKB alpha/Akt1. Biol Reprod. 2010;82(2):246–56.
57. Wu D, Zhao W, Xu C, Zhou X, Leng X, Li Y. Melatonin suppresses serum starvation-induced autophagy of ovarian granulosa cells in premature ovarian insufficiency. BMC Womens Health. 2022;22(1):474. https://doi.org/10.1186/s12905-022-02056-7.
58. Liu Y, Zhu X, Wu C, Lang Y, Zhao W, Li Y. Melatonin protects against ovarian damage by inhibiting autophagy in granulosa cells in rats. Clinics (Sao Paulo). 2022;77: 100119. https://doi.org/10.1016/j.clinsp.2022.100119.
59. Guo R, Zheng H, Li Q, Qiu X, Zhang J, Cheng Z. Melatonin alleviates insulin resistance through the PI3K/AKT signaling pathway in ovary granulosa cells of polycystic ovary syndrome. Reprod Biol. 2022;22(1): 100594. https://doi.org/10.1016/j.repbio.2021.100594.
60. Huang Y, Hu C, Ye H, et al. Inflamm-Aging: A New Mechanism Affecting Premature Ovarian Insufficiency. J Immunol Res. 2019;2019:8069898.
61. Yang H, Pang H, Miao C. Ovarian IL-1α and IL-1β levels are associated with primary ovarian insufficiency[J]. Int J Clin Exp Pathol. 2018;11(9):4711–7.
62. Jiang Y, Zhang Z, Cha L, et al. Resveratrol plays a protective role against premature ovarian failure and prompts female germline stem cell survival[J]. Int J Mol Sci. 2019;20(14):3605.
63. Garcez ML, Tan VX, Heng B, Guillemin GJ. Sodium Butyrate and Indole-3-propionic Acid Prevent the Increase of Cytokines and Kynurenine Levels in LPS-induced Human Primary Astrocytes. Int J Tryptophan Res. 2020;13:1178646920978404. https://doi.org/10.1177/1178646920978404.
64. Zheng Q, Li Y, Zhang D, et al. ANP promotes proliferation and inhibits apoptosis of ovarian granulosa cells by NPRA/PGRMC1/EGFR complex and improves ovary functions of PCOS rats [J]. Cell Death Dis. 2017;8(10): e3145.
65. Rawlings JS, Rosler KM, Harrison DA. The JAK/STAT signaling pathway. J Cell Sci. 2004;117:1281–3.
66. Shimada M, Ito J, Yamashita Y, et al. Phosphatidylinositol 3-kinase in cumulus cells is responsible for both suppression of spontaneous maturation and induction of gonadotropin-stimulated maturation of porcine oocytes. J Endocrinol. 2003;179:25–34.
67. Fan HY, Liu Z, Shimada M, et al. MAPK3/1 (ERK1/2) in ovarian granulosa cells are essential for female fertility. Science. 2009;324:938–41.

68. Liu Q, Li Y, Feng Y, et al. Single-cell analysis of differences in transcriptomic profiles of oocytes and cumulus cells at GV, MI, MII stages from PCOS patients [J]. Sci Rep. 2016;6:39638.
69. Komar CM, Braissant O, Wahli W, et al. Expression and localization of PPARs in the rat ovary during follicular development and the periovulatory period [published correction appears in Endocrinology 2001 Dec; 142(12):5320]. Endocrinology. 2001;142(11):4831–8.
70. Castoria G, Migliaccio A, Bilancio A, et al. PI3-kinase in concert with Src promotes the S-phase entry of oestradiol-stimulated MCF-7 cells. EMBO J. 2001;20(21):6050–9.
71. Rayala SK, Hollander PD, Balasenthil S, et al. Hepatocyte growth factor-regulated tyrosine kinase substrate (HRS) interacts with PELP1 and activates MAPK. J Biol Chem. 2006;281(7):4395–4403.
72. Gaetani L, Boscaro F, Pieraccini G, et al. Host and Microbial Tryptophan Metabolic Profiling in Multiple Sclerosis. Front Immunol. 2020;11:157. https://doi.org/10.3389/fimmu.2020.00157.
73. Merhi Z. Advanced glycation end products and their relevance in female reproduction. Hum Reprod. 2014;29(1):135–45.
74. Gill V, Kumar V, Singh K, et al. Advanced Glycation End Products (AGEs) May Be a Striking Link Between Modern Diet and Health. Biomolecules. 2019;9(12):888.
75. Yin QQ, Dong CF, Dong SQ, et al. AGEs induce cell death via oxidative and endoplasmic reticulum stresses in both human SH-SY5Y neuroblastoma cells and rat cortical neurons. Cell Mol Neurobiol. 2012;32(8):1299–309.
76. Park S, Kim S, Jin H, et al. Impaired development of female mouse offspring maternally exposed to simazine. Environ Toxicol Pharmacol. 2014;38(3):845–51.
77. Feugang JM, Greene JM, Willard ST, et al. In vitro effects of relaxin on gene expression in porcine cumulus-oocyte complexes and developing embryos. Reprod Biol Endocrinol. 2011;9:15.
78. Findlay JK, Liew SH, Simpson ER, et al. Estrogen signaling in the regulation of female reproductive functions. Handb Exp Pharmacol. 2010;198:29–35.
79. Gundu C, Arruri VK, Sherkhane B, Khatri DK, Singh SB. Indole-3-propionic acid attenuates high glucose induced ER stress response and augments mitochondrial function by modulating PERK-IRE1-ATF4-CHOP signalling in experimental diabetic neuropathy. Arch Physiol Biochem. Published online January 11, 2022. https://doi.org/10.1080/13813455.2021.2024577.

Publisher's Note